Mobile lidar system for environmental probing

Fredriksson, K; Galle, B; Nystrom, K; Svanberg, Sune

Published in:
Applied Optics

DOI:
10.1364/AO.20.004181

1981

Mobile lidar system for environmental probing

K. Fredriksson, B. Galle, K. Nyström, and S. Svanberg

A fully mobile remote-sensing system based on the lidar principle is described. With this system, atmospheric probing using Mie scattering, differential absorption, or Raman techniques can be performed yielding information on atmospheric pollutants or general atmospheric parameters. The system incorporates a powerful Nd:YAG laser pumping a dye laser and is equipped with a fixed Newtonian telescope used in conjunction with a flat steering mirror. The lidar signals are electrically recorded using a fast-transient digitizer and are processed by a minicomputer, which also controls the laser, the chosen measuring direction, and the output media. Examples of measurements on atmospheric NO_2 and SO_2 are given.

I. Introduction

Remote sensing of environmental parameters using laser techniques has proved to have great potential. Atmospheric probing using long-path absorption or lidar methods have been performed by several groups. Hydrospheric measurements employing lasers have been less extensive so far. Besides bathymetric work, interest has been focused on laser-induced fluorescence in pollutants and algae. The research activities with regard to air as well as water have been discussed recently by Measures[1] and Svanberg.[2] Some of the laser techniques for environmental probing are now approaching a state of operationality with the development of powerful computer-controlled equipment. In this department remote-sensing experiments using lasers were initiated in 1975. Atmospheric probing with lidar techniques was described in a recent paper.[3] Experiments related to hydrospheric probing were described, e.g., in Refs. 4 and 5. Parallel with an extensive field test program in which mainly laboratory equipment was used, our research group has been involved in the definition process for a dedicated laser remote-sensing system.[6,7] This work has been sponsored by the Swedish Space Corp. and the Swedish Board for Space Activities. In early 1979 the group received a grant from the Swedish Space Corp. for developing a dedicated measuring system intended for research but also for routine monitoring. In the present paper we will describe the lidar system and give examples of its measuring capabilities.

II. Lidar Technique

In a lidar system, where the beam from a pulsed laser is transmitted into the atmosphere, the backscattered laser light from a distance R is collected with a time delay $t = 2R/c$, where c is the velocity of light. The power $P_\lambda(R,\Delta R)$ from a length interval ΔR at the distance R is given by the general lidar equation, which can be expressed in a simplified way as

$$P_\lambda(R,\Delta R) = CW\sigma_b N(R)\frac{\Delta R}{R^2} \times \exp\left\{-2\int_0^R [\sigma(\lambda)n(r) + \sigma_a N(r)]dr\right\}. \quad (1)$$

Here C is a system constant, W is the transmitted pulse power, $N(R)$ is the number of scattering objects per unit volume, and the exponential factor describes the attenuation due to molecules and particles of concentration $n(r)$ and $N(r)$, with absorption cross sections σ and σ_a, respectively. The lidar equation, Eq. (1), is here given in a condensed form, where summations over molecules and particles are assumed and the wavelength for the detection is the wavelength of the transmitted laser light. A more extensive expression of the general lidar equation is discussed in Ref. (8).

The elastically back scattered light in the visible and the IR is almost exclusively due to Mie scattering from particles. Thus, the Mie scattered lidar signal can be

When this work was done all authors were with Chalmers University of Technology, Physics Department, S-412 96 Göteborg, Sweden; K. Fredriksson is now with National Swedish Environment Protection Board, Studsvik, S-611 82 Nyköping, Sweden; B. Galle is with Institute for Air & Water Research, Box 5207, S-402 24 Göteborg, Sweden; K. Nyström is with Myab AB, Heurlin Plats 1, S-413 01 Göteborg, Sweden; and S. Svanberg is with Lund Institute of Technology, Physics Department, Box 725, S-220 07 Lund, Sweden.

Received 4 June 1981.
0003-6935/81/244181-09$00.50/0.

used for mappings of particle concentrations. In certain situations calibrations can be done with other measurement techniques, and then also quantitative measurements can be performed.

The Raman backscattering, which is a nonelastic scattering process, is usually very weak. In certain cases, when gases of high concentrations are to be measured, a high-power fixed-frequency lidar system can be useful. So far, the most useful applications of the Raman techniques for atmospheric studies have been measurements of humidity and also atmospheric temperature, where the dependence of the Raman line profiles with the temperature has been studied.

In the differential absorption lidar (DIAL) technique the differential absorption by a molecular constituent is studied. A tunable laser is adjusted to an absorption wavelength λ_{abs} of the molecule, and the lidar signal according to Eq. (1) is compared with the signal at a reference off-line wavelength λ_{ref}:

$$\frac{P_{\lambda_{abs}}(R)}{P_{\lambda_{ref}}(R)} = C' \cdot \exp\left\{-2 \int_0^R [\sigma(\lambda_{abs}) - \sigma(\lambda_{ref})] n(r) dr\right\}, \quad (2)$$

where C' is a new system constant. Here the $P(R)$ signal functions must be corrected for background. When the studied gas is present, expressed by the factor $n(r)$ in Eq. (2), $P_{\lambda_{abs}}/P_{\lambda_{ref}}$ will decrease with the distance, and the slope is determined by the gas concentration. The DIAL technique has proved very useful for measurements of constituents in the atmosphere such as gaseous pollutants and water vapor. Examples of such measurements were given in Ref. 3. Other works are listed in Refs. 1–3 and 8.

The induced fluorescence following on laser excitation can in some cases be used in the lidar technique. The applications for atmospheric studies are limited because of quenching and other physical effects in the troposphere. However, the induced fluorescence from liquid and solid targets can be studied in a favorable way as was discussed in Ref. 4. Probing of the sea surface layer can be made for the detection of, e.g., oil spills and algae blooms. In Ref. 4 an extensive study of the characteristic fluorescence properties of different materials was performed.

III. Lidar System Description

In this section we will describe the mobile lidar system. We will separately treat the system platform, the laser system, the detection telescope and optical system, detection electronics and minicomputer, and finally the system steering. In Fig. 1 a photograph of the system is shown. For a general description we refer to Figs. 2 and 3.

A. System Platform

The platform for the mobile lidar system is a covered truck with a total weight of 3500 kg. The walls and roof of the truck cargo compartment have been reinforced by several steel-profile arches to allow a rigid mounting of the different units of the lidar system. A schematic of the system displaying the layout of the cargo compartment is shown in Fig. 2. Along one long wall, one

Fig. 1. Mobile lidar system.

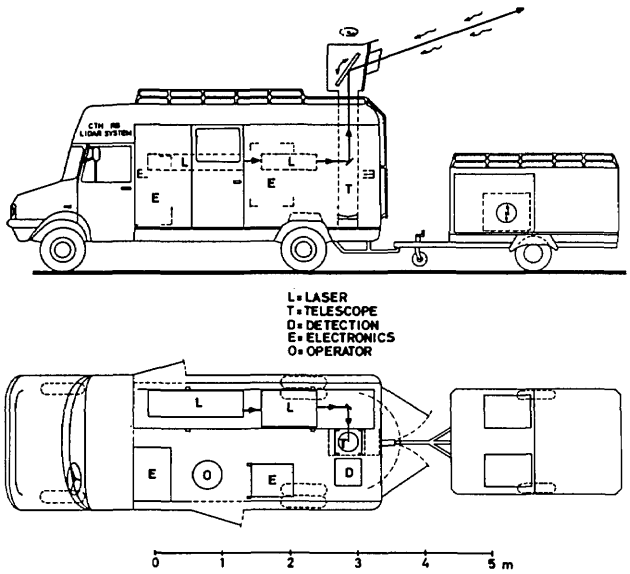

Fig. 2. Schematic of mobile laboratory.

or two benches, 350 × 60 cm, can be mounted on four vertical poles, the ends of which are equipped with springs and rubber steerings extending into tube-shaped mounts fixed to the floor and the arch structure. In this way an efficient shock absorption and vibration isolation are obtained. End sections (60 × 50 cm) of the benches can be removed to add flexibility to the system. The benches can be mounted at chosen heights and locked into operational position by pintles. The detection telescope and the main electronic bay are mounted with the same type shock absorber and vibration isolator. A sliding door connects the laboratory space, 3.60 (length) × 1.90 (width) × 1.85 m (height), with the driver's cabin. The truck can be stabilized by four jacks welded to the chassie. The stabilized platform allows lidar pointing accuracies of the order of 0.5 mrads. A covered trailer accommodates two 5-kW motor generators. The two-stroke engines are equipped with four 25-liter gasoline tanks providing 12 h of operation.

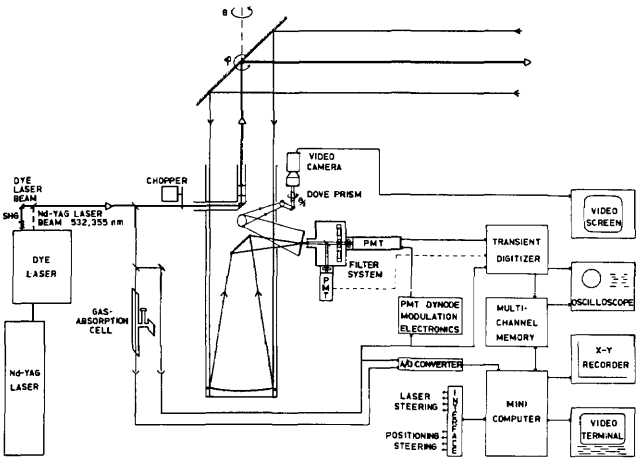

Fig. 3. Optical and electronic arrangements of lidar system.

The comparatively small but rigid system platform has turned out to be well suited for fieldwork. The system can be transported at high speed, and the setup time for the measurements is less than half an hour.

B. Laser System

The primary laser of the system is a Nd:YAG laser unit (Quanta-Ray DCR-1), producing 250-mJ pulses at 1.064 μm at a normal repetition rate of 10 Hz. The laser can be frequency doubled or tripled with a pulse energy of 100 and 50 mJ, respectively. The pulse length is typically 7 nsec in the normal Q-switched operation. The shorter wavelength outputs can be used to pump a tunable dye laser (Quanta-Ray PDL-1), which consists of a grating- tuned oscillator and one or two amplifier stages. Rhodamine dyes are operated with one amplifier only, whereas both stages are used when coumarin dyes are employed. All the optics that must be moved or adjusted when the dye is changed are accessible from the outside of the dye laser. Thus, the dustproof cover of the laser can be kept on the laser during fieldwork. A linear tuning with readout on a DIAL scale is obtained by using a sine drive operated either manually or using a stepper motor. For achieving a rapid wavelength shift between the laser pulses the sine-drive push plate is split into two parts connected by a joint. The edge of the push plate can then be moved periodically through the action of an excenter wheel, rotated by means of a stepper motor. The laser is fired after every half turn of the excenter wheel, and the phase angle determines the corresponding wavelength change, which can be varied between 0 and ~40 Å. By properly adjusting the sine-drive setting and the phase angle of the excenter wheel, a small well-defined change of the wavelength between alternating laser shots can be accomplished for DIAL measurements. The output of the dye laser can be frequency doubled using one of several KD*P nonlinear crystals, which can be phase matched by angle-tuning over given wavelength intervals. Each crystal is hermetically sealed and mounted on a rotary stage, which can be periodically turned by the action of a further excenter wheel driven by a stepper motor. This wheel is normally driven in synchronism with the wavelength-controlling wheel, and the phase angle of the doubling crystal wheel is adjusted to achieve phase matching at both the used wavelengths. A second crystal of the same type is planned to be included in the system. This will be mounted after the other crystal. The two crystals will then in a DIAL measurement be individually tuned to the absorption and reference wavelengths, respectively. This will, of course, reduce the laser power but may be favorable to use in some cases where it is critical that the laser power be kept at a constant level. It will certainly be easier to adjust.

A UV-transmitting filter is used to suppress the visible output from the dye laser while transmitting the UV radiation. Likewise, a dichroic mirror can be used for splitting off the 1.064-μm radiation of the pump laser into a radiation dump to keep all IR radiation inside the pump laser. The Nd:YAG laser has a closed-loop cooling system with separate compressor and radiator units. Two dye circulator units are placed under the laser bench. Each unit has separate loops for the oscillator and amplifier systems.

C. Optical Systems

We shall now describe the optical systems besides the laser transmitter. These are displayed in Fig. 3, where a schematic setup of the lidar system is given. The laser pulses, either from the Nd:YAG laser directly or from the dye laser, are reflected toward the measuring volume using a number of optical components. First the beam is deflected 90° using a quartz right-angle prism. About 5% of the beam is split off by a quartz plate and further reflected 90° into a calibration-cell unit mounted below the laser bench. Inside the unit the beam is split by a 50% coated quartz plate into two beams of approximately equal intensities. One beam passes a calibration cell before arriving at a photodiode, whereas the other beam directly arrives at a photodiode of the same type. The calibration cell is made of quartz, with two interconnected absorption tubes of 30- and 6-cm length, respectively. By using the proper path length a suitable absorption can be obtained for a given gas concentration. The absorption tubes have Brewster windows, and the assembly can be filled through Teflon valves. The cell can be mounted in two ways to be useful for both vertically and horizontally polarized light. Neutral density filters are placed in front of the detectors to obtain a proper operation range.

The main part of the laser beam is sent through a tube to the axis of the system telescope, where it is vertically deflected by a right-angle quartz prism. This prism can be accurately tilted in two directions by adjustment screws extending outside the telescope for convenient operation. The laser beam can be expanded 5 times from an original 7-mm diam to 35-mm diam using a quartz Galilean beam expander mounted on the telescope axis. The original laser beam has an adequately low beam divergence, 0.7 mrad, and the main reason for introducing the expander is to protect the aluminum

coating of the large 60- × 30-cm beam-director mirror mounted in the transmission/reception dome. The expander can also be used for diverging the laser beam, decreasing the safety range when visible radiation is used. The laser beam leaves the lidar truck through a 50- × 30-cm Herasil quartz window providing full weather protection for the system. The window can be heated by a stream of hot air blown by a fan. An elongated detachable tube mounted in front of the window protects the quartz surface from precipitation.

Light backscattered from the measurement volume enters the system through the same quartz window and is deflected down into the telescope by the plane dome mirror. The vertical movement of the mirror is controlled by a stepper motor. For choosing the horizontal positioning, the whole dome arrangement is turned by another stepper motor. The dome is mounted using large counterloaded ball bearings. Metal flanges and a rubber flange provide a watertight connection between the turning dome and the lidar truck. The received backscattered light is focused by a 30-cm diam $f/3.3$ spherical mirror with aluminum coating and a UV-enhanced protective layer. A Newtonian plane mirror placed on the telescope axis is used for deflecting the focusing light toward the detection unit. In the focal plane a slightly inclined metal mirror is placed, reflecting the light toward the visual inspection system. In the center of the metal mirror a hole is drilled, through which passes the light to be detected. Clearly, this aperture defines the field of view of the telescope, which will be 1 mrad for a 1-mm diam hole. It should be chosen to match the laser beam divergence. A set of mirrors with different holes can be used for different applications. In addition, an iris aperture is placed behind the mirror hole. This iris can be used to determine the effective divergence of the laser beam by increasing the aperture until no further signal increase occurs. After the iris, the beam is made parallel using an f = 10-cm quartz lens. The parallel beam passes a graded beam splitter, where a chosen fraction of the light can be split off at 90° to arrive at an EMI 9817 photomultiplier tube after optical filtering. The main beam passes through a filter position, where one out of eight filters or filter combinations mounted on a filter wheel is placed. The filter wheel is turned by a stepper motor. The filtered light is detected by a further EMI 9817 photomultiplier tube equipped with dynode modulation.

Light reflected by the metal mirror in the focal plane of the main telescope is once more reflected by a mirror placed between the beam director prism and the Newtonian mirror into a visual inspection unit, where after further reflections the light passes a Dove prism, which inverts the image. The light then passes into a video camera with a teleconverter lens, producing a sharp image of the surveyed area on a 22.5-cm (9-in.) video screen. As the metal mirror is in the focal plane of the telescope mirror, the detection aperture appears sharp in the center of the picture. Thus, it is very easy to locate the exact position of the probing beam. When the transmitter/receiver dome is rotated, the horizon of the video picture will normally also rotate. The remedy for this is to rotate the Dove prism at half the angle velocity of that of the dome movement.

D. Detection Electronics and Minicomputer

In the photomultiplier tube the optical signal is converted into an electrical transient of short duration. In the case of a very weak signal, a set of preamplifiers may be used. Atmospheric backscattering from the lidar system out to a range of 3 km corresponds to a transient duration of 20 μsec. The fast transient is captured with a Biomation 8100 transient digitizer, which has a maximum of 2048 time channels with a minimum separation of 10 nsec. It has an 8-bit analog to digital converter. The transient digitizer keeps a stored record of the transient, which is displayed on the system oscilloscope. The digitized transient is also rapidly transferred to a specially designed multichannel memory, which operates at a 24-bit word length. The transient is stored in one of eight 2048-channel memory sections. Each of these sections can be divided into eight 256-channel subsections, which can be used if a record of full length and time resolution is not required. The sum curve is displayed on a second channel of the oscilloscope so that the signal improvement can be followed together with the individual transients. The main use of the multichannel memory is in connection with the system minicomputer, through which the section in use and the number of averaged transients normally are chosen. The averaged signal is transferred into the minicomputer for further processing. The multichannel memory thus serves as an external memory, where the fast averaging operations are performed in hardware, while the slower further processing is performed in the minicomputer using proper software.

The system computer is a PDP 11 V03 unit with a 60-kbytes memory. Two floppy disk systems, each with a memory capacity of 512 kbytes/disk, are used. One disk is used for the software governing the possible measuring routines, while the other one is used for the storage of data. Interaction with the operator is provided through a video terminal. Hard copies of graphs representing measurement data can be obtained from a computer-controlled X-Y recorder.

E. System Steering

In Fig. 4 a signal flow chart diagram for the lidar system is shown. The whole measuring system can be controlled by the minicomputer via a DRV-11 interface. The computer interacts with the different subsystems via stepper-motor drivers, digital to analog converters, and trigger signals. In this way a long complicated measuring program can be performed automatically without operator interference. Two stepper motors control the vertical and horizontal movements of the transmitting/receiving mirror. A third stepper motor, synchronized with the horizontal movement, controls the rotation of the Dove prism. As the mirror is moved, ten-turn potentiometers are also turned using proper

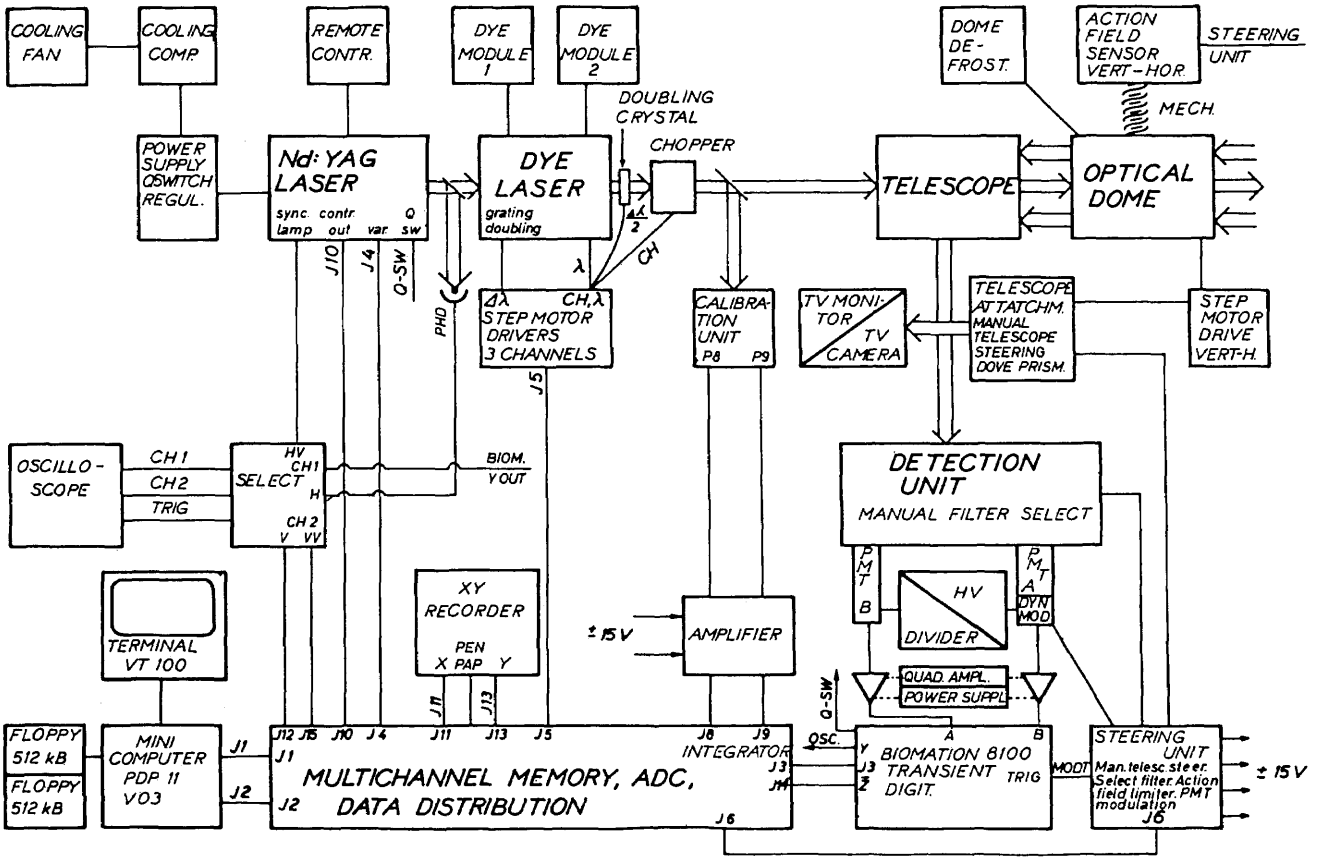

Fig. 4. Signal flow chart diagram.

gears, providing reference voltages for the mirror position. These voltages are then compared with upper and lower voltages set manually to provide limits outside of which mirror movements are suppressed. In this way shooting boundaries can be set both horizontally and vertically, which provides safety when the system is operated in a way so that eye-safety considerations apply. Separate pulse generators enable manual operation of the mirror at variable sweep speeds both from the operator's chair and from the telescope assembly.

The filter wheel of the detection unit is operated using a further computer-controlled stepper motor. The eight filter positions can also be chosen manually both from the operator's chair and from the detection unit. At both places LEDs indicate which filter is currently in position.

The laser firing is also controlled by the computer. Stepper-motor drivers for the excenter wheels of the dye laser, used for changing the wavelength and the phase-matching angle, respectively, and for the setting of the primary grating angle enable full computer control of the dye laser. A chopper driven by a stepper motor can be used to block every fifteenth and sixteenth pulse during a measurement cycle. The detection electronics are also activated during this pulse, and after multiplication the averaged signal from the blank shots can be used for subtracting the background from the lidar signal. Apart from correcting for the ambient light level and providing a true zero level for the signal amplitude measurement, this feature is also very useful for eliminating possible laser-induced rf interference.

The lidar signal varies strongly with the range R (an approximate $1/R^2$ signal falloff). This can cause problems because of the limited dynamic range of the fast-transient digitizer. In this system these problems are partly overcome by geometrical compression in the design of the optical system, as discussed by Harms *et al.*[9] Electronic modulation of the photomultiplier dynode-chain voltage is also employed. The modulation is triggered by the laser shot and implies a shaped voltage increase with time, increasing the amplification of the photomultiplier tube. In this way the weak lidar signal at larger distances is more efficiently collected by the transient digitizer. The photomultiplier dynode chain is similar to that described by Allen and Evans.[10] The measurement data arrive at the computer via the multichannel memory. Further, the signal levels from the photodiodes of the calibration unit are digitized and fed into the computer. The analog signals can also be displayed on the oscilloscope as well as the signal from a photodiode, monitoring the Nd:YAG laser pulse for proper setting of the Q-switch timing and holdoff. A switching box provides fast interchange of the signals on display on the oscilloscope as well as trigger signals

from the proper sources. The computer software is made up of a large number of subroutines that are combined with a main program for the steering of the system, the collecting of the lidar data, and the calculation procedures. The complete program has a size of ~52 kbytes. The same main program is used for mappings of aerosols, DIAL and Raman measurements, and for fluorescence studies. The different characteristics for the typical measurement performed is chosen by calling the proper set of subroutines. We have found it customary to work with such a large program instead of using smaller individual programs for different types of measurements. The program is built up with a set of questions to the operator, where the terminal is the communicating medium. In this way the computer program can be easily understood and run by a nonspecialist.

An example of the computer program structure for the steering of the system and storing of the lidar data is shown in Fig. 5. Part of the program flow chart is displayed in the figure. Interrupt routines are used in the program, and this increases the measurement capabilities very much. The settings of the wavelength and UV-tracking are continuously changed by the rotation of the excenter wheels discussed in a previous section. The laser is triggered at a preset position of the wavelength wheel and also at 180° from this position. The chopper wheel is turned synchronously with the laser triggering, and the laser is blocked each fifteenth and sixteenth laser shots. Three memory sections in the multichannel memory, each consisting of 2048 channels, are used for the storing of the absorption and reference wavelength measurements and the background recording. In the same time as the data recording is made, two former measurements in another measurement direction are read from the diskette memory sections. In the figure these former measurements are labeled *FILE B*. When a preselected number of measurement cycles, each consisting of sixteen laser pulses, is completed, the measurement direction is changed by the computer. During this operation the laser is blocked. The data averaging is then continued for the measurement B at the same time as the background is subtracted from the completed measurement recordings. Before the background is subtracted it is smoothed with a Gaussian function, except for the first eighth part. The reason for not smoothing the first part is that any rf interference should not be smoothed but completely subtracted from the measurement. In the latter parts of the background recording, the signal is completely made up of randomly spread photon counts, and thus a smoothing procedure is desired. After multiplying the background for compensating for the fewer recordings, it is subtracted from the two measurements, and these are then stored on the diskette memory. In the figure these measurements are stored with the label *FILE A*. After this, two other measurements are read from the diskette memory into the first two memory sections, and the same cycle is repeated. With the program sketched here it is possible to do DIAL measurements in up to thirty directions chosen sequentially in a repeated cycle. The time for one data recording cycle in one direction is ~40 sec and consists of 175 lidar recordings at the absorption and reference wavelengths.

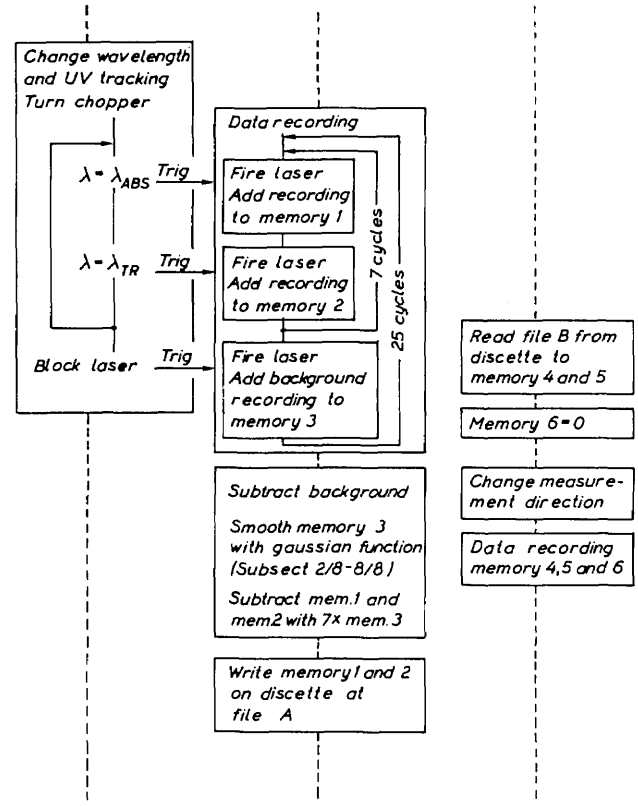

Fig. 5. Part of the computer program for DIAL measurements. Program structure is made up of interrupt routines.

The computer main program is also used for the evaluation of the measurement result, either as a displayed curve or in concentration numbers. The program includes a large number of calculation programs, e.g., programs for smoothing with a selectable Gaussian function, logarithmic operations, and routines for evaluation of DIAL recordings into $\mu g/m^3$ of the studied gas.

IV. Examples of Measurements

The mobile system has been operated for a half-year period at the Air Laboratory of the National Swedish Environment Protection Board. Several field tests have been performed in which aerosols, nitrogen dioxide, and sulfur dioxide were measured. These measurements and the experiences from the fieldwork will be presented in forthcoming papers. Here a few examples will be discussed to illustrate some of the measurement capabilities of the mobile system.

Figure 6 displays a typical example of a DIAL measurement of nitrogen dioxide in a smokestack plume. The mobile system was in this case placed at a distance of 1350 m from the studied smokestack of a saltpeter plant. Three measurement directions just above the

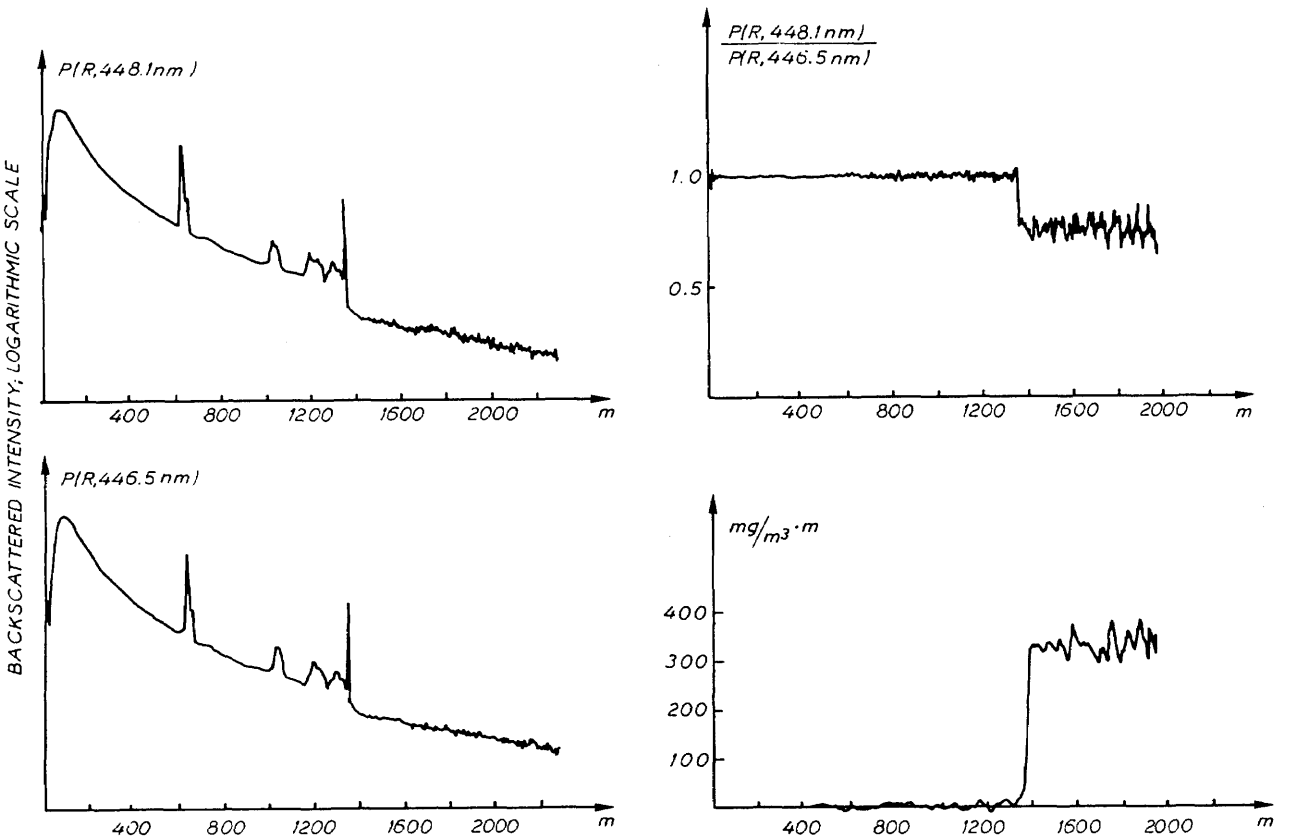

Fig. 6. Nitrogen dioxide DIAL measurement of a smokestack plume. Lidar is pointed just above the top of the smoke stack at a distance of 1350 m. Two lidar signals are shown to the left, and the DIAL curve is displayed at the upper right in the figure. Nitrogen dioxide is integrated across the plume and is shown as a step in the lower right curve.

top of the 3-m wide stack were chosen for the determination of the total concentration. One of the measurements is shown in the figure. The time for a complete measurement cycle was 13 min. The lidar recordings at the 448.1-nm NO_2 absorption wavelength and the 446.5-nm reference wavelength are displayed in a logarithmic scale. The curves are the averaged recordings from 1050 laser-pulse pairs of rather low energy, 2 mJ/pulse. As can be seen, the atmosphere is very inhomogeneous with several plumes. The background recordings were subtracted from the lidar curves during the measurement according to the routine discussed above. The divided DIAL curve $P(R,448.1)/P(R,446.5)$ is also shown in the figure. In this curve the dependence of the particle contents is eliminated. The figure clearly shows that even in a situation with rather heavy aerosol plumes one gets a satisfactory result when the absorption and reference wavelengths are measured one-tenth of a second apart. From the DIAL curve the integrated nitrogen dioxide concentration was calculated using the absorption cross sections published by Woods and Jolliffe.[11] The value was found to be 366 $mg/m^3 \cdot m$, which is expected to be good within 20%. The accuracy is mainly limited by an uncertainty in the absorption cross sections. From this, the NO_2 concentration in the plume was calculated to be 122 ± 30 mg/m^3 using the known stack diameter. This value was compared to a calculation made from an in-stack measurement performed with a conventional method that yielded the value 120 mg/m^3, although with low accuracy. The gas outlet was 13 m/sec, which was measured in the stack, and the total NO_2 outlet was then determined to be ~40 kg/h on this special occasion.

An example of a sulfur dioxide measurement is shown in Fig. 7. This is a measurement above the top of a smokestack at a cement plant. The recordings are the averaged results from 980 laser-pulse pairs at the 300.05-nm absorption wavelength and the 299.30-nm reference wavelength. In the DIAL curve the particle dependence is not as nicely eliminated as in the former example due to the problem of achieving a constant UV tracking when the laser wavelength is changed ten times per second. In this case, however, when a smoke plume is studied, this is obviously not a severe limitation. When ambient air concentrations are to be measured, a slight modification of the UV-tracking system is needed, as was discussed previously. The sulfur dioxide content in the example shown was calculated using the absorption cross sections measured by Jolliffe and Woods.[12] The integrated concentration was found to be 270 $mg/m^3 \cdot m$, with an accuracy of 20%, which also in this case is limited by an uncertainty of the absorption cross-section values and the measurement wavelengths. The sulfur dioxide concentration in the plume was found to be 84 ± 17 mg/m^3 from the complete measurement cycle.

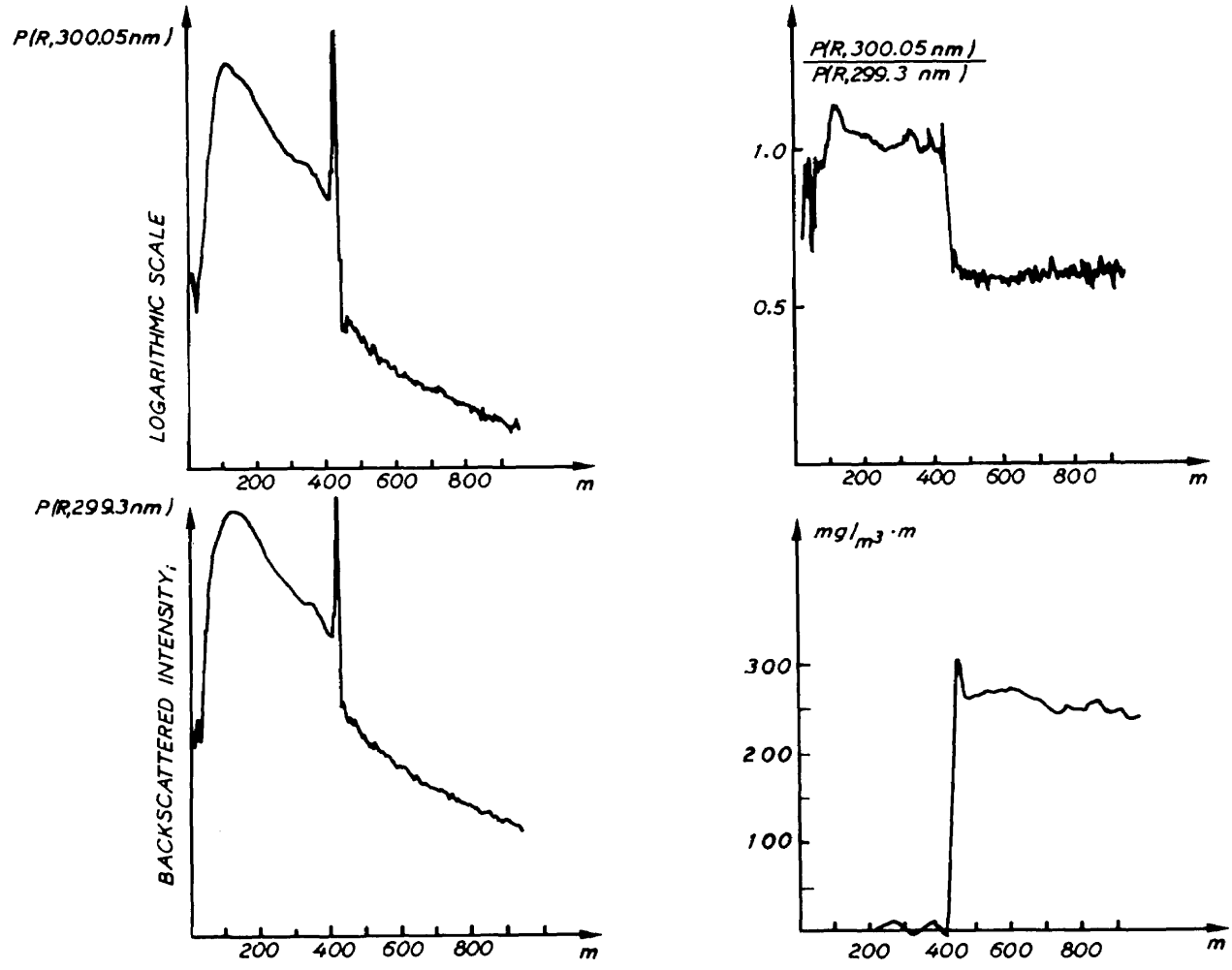

Fig. 7. DIAL measurement of sulfur dioxide content in a smokestack plume from a cement plant. Lidar signals, divided DIAL curve, and integrated sulfur dioxide content as a function of the distance are shown.

Another example of a sulfur dioxide measurement is shown in Fig. 8. In this case, the diffuse emission of SO_2 from a paper mill was studied. Several measurements in different directions close to the paper mill were performed to get an idea of the total SO_2 burden from the mill. In the example shown, the lidar was directed through the paper mill area at a distance of slightly more than 1 km. The measurement curves and the calculated DIAL curve are shown in the figure. As can be seen, the atmosphere was in this case more homogeneous without any heavy plumes, and the UV-tracking system did not cause any anomalies in the DIAL curve. From the DIAL curve the SO_2 concentration was calculated with linear averaging over a 100-m long continuously sliding range interval. The curve is displayed in the lower right part of Fig. 8. Here the concentration as a function of the distance is shown, whereas in Figs. 6 and 7, where only one plume was studied, the integrated concentration with the distance was shown. The accuracy in this measurement is expected to be better than 15 $\mu g/m^3$ at <1500-m distances.

V. Conclusions

The mobile laser radar system described has proved to be powerful in monitoring remotely atmospheric pollutants such as particles NO_2 and SO_2. The system is now operational in monitoring these pollutants. Work on O_3 is in progress and appears promising. The testing and evaluation phase of this lidar project for measuring these pollutants will continue for one more year at the National Swedish Environment Protection Board. The experiences and conclusions from the work will then be published in a report from which decisions will be made on the construction of lidar systems for routine monitoring. However, the lidar system also serves as a national platform for research and development of laser techniques for atmospheric and hydrospheric probing. At present, techniques for extending the available wavelength region of the laser system are being developed at Lund Institute of Technology. Stimulated Raman shifting of the dye laser output into the VUV and near-IR regions is performed in high-pressure H_2 gas. The efforts are directed

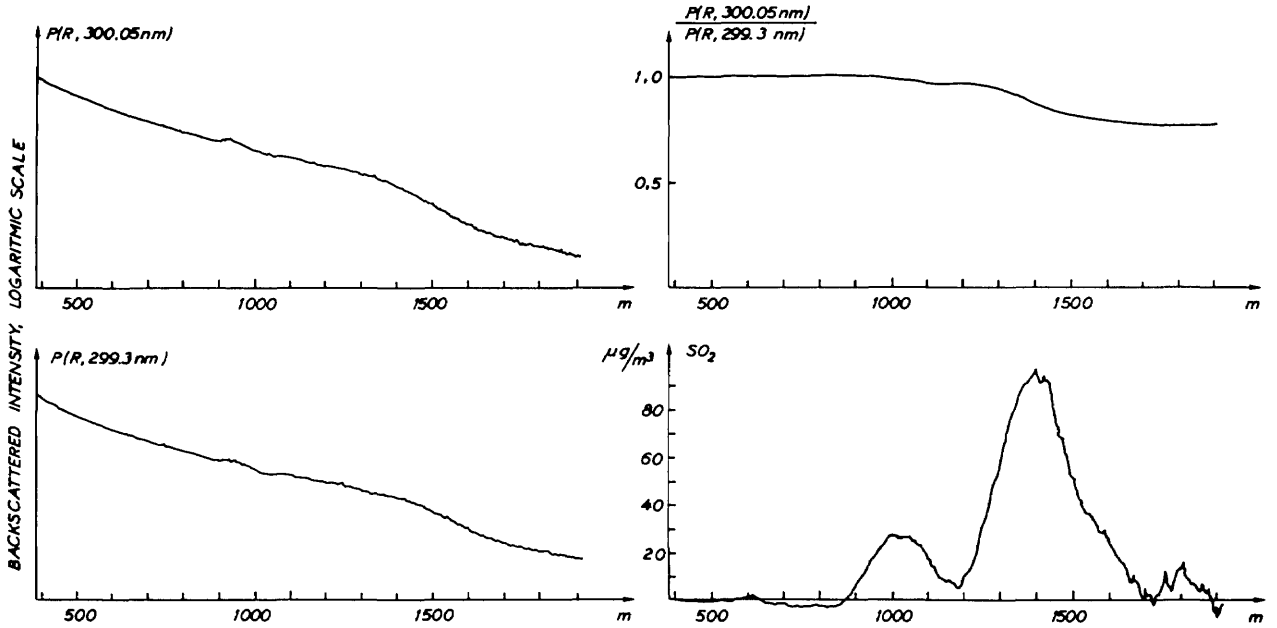

Fig. 8. Measurement of diffuse emission of sulfur dioxide at a paper mill. Lidar signals and DIAL curve are shown, together with the DIAL evaluated concentration as a function of distance. Concentration curve was evaluated with a distance resolution of 100 m, which was adequate in this case.

toward the extension of the measurement capabilities of the lidar system to include gases such as Hg, HCHO, HCl, CO, and CH_4. Meteorological measurements such as vertical sounding of water vapor profiles using Raman scattering have also been successfully performed with the mobile lidar system.[13] Experiments with laser-induced fluorescence and lidar bathymetry will also be initiated aiming at an assessment of the measurement capabilities of an airborne laser sensor.

The authors gratefully acknowledge the support from C. Pilo and C. G. Borg, Swedish Space Corp., and the interest and encouragement from G. Persson, National Environment Protection Board, and the constant support from I. Lindgren at our university. One of the authors (K. F.) is also very grateful for the support from many persons during the measurement activities, including O. Killingmo, National Environment Protection Board, T. C. Berg and J. Schjoldager, Norwegian Institute for Air Research, and H. Edner, Lund Institute of Technology.

The grant for the development phase was provided by the Swedish Space Corp., and the grants for the continuing research activities are provided by the Swedish Space Corp. and the National Environment Protection Board.

References

1. R. M. Measures, in *Analytical Laser Spectroscopy*, N. Omenetto, Ed. (Wiley, New York, 1979).
2. S. Svanberg, Contemp. Phys. **21,** 541 (1980).
3. K. Fredriksson, B. Galle, K. Nyström, and S. Svanberg, Appl. Opt. **18,** 2998 (1979).
4. L. Celander, K. Fredriksson, B. Galle, and S. Svanberg, Göteborg Institute of Physics Reports GIPR-149 (1978).
5. K. Fredriksson, B. Galle, K. Nyström, S. Svanberg, and B. Öström, Göteborg Institute of Physics Reports GIPR-162 (1978).
6. E. Almqvist and S. Svanberg, *Investigation on Operational Systems for Remote Sensing of Air- and Water-Pollutants* (Swedish Space Corp., Solna 1977) (in Swedish).
7. K. Fredriksson, B. Galle, K. Nyström, and S. Svanberg, unpublished report, 1978 (in Swedish).
8. K. Fredriksson, "Laser Spectroscopy Applied in Studies of Alkali-atom Structures and in Environmental Monitoring," Ph.D. dissertation, U. Gothenburg (1980).
9. J. Harms, W. Lahmann, and C. Weitkamp, Appl. Opt. **17,** 1131 (1978).
10. R. J. Allen and W. E. Evans, Rev. Sci. Instrum. **43,** 1422 (1972).
11. P. T. Woods and B. W. Jolliffe, Opt. Laser Technol. **10,** 25 (1978).
12. B. W. Jolliffe and P. T. Woods, Abstract, Ninth International Laser Radar Conference, Munich, DFVLR, 1979.
13. K. Fredriksson and A. Hågård, to be published.